Biomedicine & Pharmacotherapy 156 (2022) 113942

Contents lists available at ScienceDirect

Biomedicine & Pharmacotherapy

journal homepage: www.elsevier.com/locate/biopha

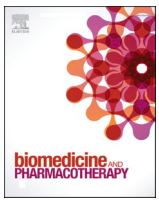

# AZ12756122, a novel fatty acid synthase inhibitor, decreases resistance features in EGFR-TKI resistant EGFR-mutated NSCLC cell models

Emma Polonio-Alcalá [a,b], Rut Porta [a,c], Santiago Ruiz-Martínez [a], Carmen Vásquez-Dongo [a,d], Joana Relat [e,f,g], Joaquim Bosch-Barrera [c], Joaquim Ciurana [b,*], Teresa Puig [a,**]

[a] New Therapeutic Targets Laboratory (TargetsLab)-Oncology Unit, Department of Medical Sciences, University of Girona, Spain
[b] Product, Process and Production Engineering Research Group (GREP), Department of Mechanical Engineering and Industrial Construction, University of Girona, Spain
[c] Medical Oncology Department, Catalan Institute of Oncology, Spain
[d] Department of Pathology, Dr. Josep Trueta University Hospital, Spain
[e] Department of Nutrition, Food Sciences and Gastronomy, School of Pharmacy and Food Sciences, Food Torribera Campus, University of Barcelona, Spain
[f] Institute of Nutrition and Food Safety of the University of Barcelona (INSA-UB), Spain
[g] CIBER Physiopathology of Obesity and Nutrition (CIBER-OBN), Instituto de Salud Carlos III, Spain

ARTICLE INFO

*Keywords:*
NSCLC
FASN
EGFR
Osimertinib
Drug combination

ABSTRACT

Different EGFR tyrosine kinase inhibitors (TKIs) have been developed for the treatment of non-small cell lung cancer (NSCLC) patients harboring sensitizing mutations in the EGFR gene. Apart from acquired secondary mutations, multiple resistance mechanisms have been reported, such as the overexpression of fatty acid synthase (FASN), a multi-functional enzyme essential for the *de novo* lipogenesis, or the increase of cancer stem cells, a small subpopulation within the tumor responsible for relapse, metastasis, and resistance to therapies. Hence, the purpose of this work is to evaluate the novel FASN inhibitor AZ12756122, both alone and in combination with gefitinib and osimertinib, in EGFR-mutated (EGFRm) lung adenocarcinoma cell models sensitive and resistant to EGFR-TKIs. The molecular effect of AZ12756122 (alone and in combination with EGFR-TKI) on FASN, EGFR/STAT3, Akt/mTOR, and MAPK signaling pathways was analyzed using RT-qPCR and Western blot. FASN expression was also evaluated in samples from patients with EGFRm NSCLC through immunohistochemistry. Our findings revealed that AZ12756122 caused cytotoxic effects inducing apoptosis, downregulated FASN expression and activity, decreased the activation of EGFR and Akt/mTOR pathway, and reduced cancer stem-like cells. Furthermore, the combination of AZ12756122 and osimertinib sensitized cells to EGFR-TKI, showing a synergistic effect that resulted in a reduction in the activation of EGFR, Akt/mTOR, and MAPK signaling pathways. Our study also showed that FASN+ EGFRm NSCLC patients exhibited a longer mPFS in patients who responded to EGFR-TKI treatment. In conclusion, FASN inhibition should be further studied for the treatment, alone or in combination with EGFR-TKIs, for EGFRm NSCLC patients.

## 1. Introduction

Lung cancer is the second most common cancer diagnosed and the first leading cause of cancer-related death. In 2020, more than 2.2 million new cases were reported and approximately 1.8 million deaths were recorded worldwide in both sexes, according to the World Health

*Abbreviations:* CSCs, Cancer Stem Cells; CI, Combination Index; EGFR, Epidermal Growth Factor Receptor; FASN, Fatty Acid Synthase; $IC_{50}$, Half-maximal Inhibitory Concentration; IHC, Immunohistochemistry; GR, Gefitinib-Resistant; LC3, Light Chain 3; mPFS, Median Progression-Free Survival; NSCLC, Non-Small Cell Lung Cancer; PARP, Poly (ADP-Ribose) Polymerase; STAT3, Signal Transducer and Activator of Transcription 3; TKI, Tyrosine Kinase Inhibitor.

* Correspondence to: Product, Process and Production Engineering Research Group (GREP), Department of Mechanical Engineering and Industrial Construction, University of Girona, 17003 Girona, Spain.

** Correspondence to: New Therapeutic Targets Laboratory (TargetsLab)-Oncology Unit, Department of Medical Sciences, University of Girona, Girona 17003, Spain.

*E-mail addresses:* emma.polonio@udg.edu (E. Polonio-Alcalá), rporta@iconcologia.net (R. Porta), santiago.ruiz@udg.edu (S. Ruiz-Martínez), cavasquez.girona.ics@gencat.cat (C. Vásquez-Dongo), jrelat@ub.edu (J. Relat), jbosch@iconcologia.net (J. Bosch-Barrera), quim.ciurana@udg.edu (J. Ciurana), teresa.puig@udg.edu (T. Puig).

https://doi.org/10.1016/j.biopha.2022.113942
Received 6 September 2022; Received in revised form 25 October 2022; Accepted 26 October 2022

Organization [1]. The most frequent subtype is non-small cell lung cancer (NSCLC), and around 40% of all lung cancer cases are classified as adenocarcinoma.

Sensitizing mutations in the tyrosine kinase domain of the epidermal growth factor receptor (EGFR) gene are frequently found in adenocarcinoma and most patients with these mutations are female and non-smokers [2–4]. The most common mutations are the exon 19-deletion (delE746_A750) and the L858R exon 21-point mutation, which together account for 90% of all EGFR mutations [4]. EGFR tyrosine kinase inhibitors (EGFR-TKIs) were designed as targeted therapy against these tumors [3]. In 2003, the Food and Drug Administration (FDA) approved the first EGFR-TKI, gefitinib, to treat patients with locally advanced or metastatic EGFR-mutated (EGFRm) NSCLC for whom chemotherapy has failed [5,6]. Despite the good response to the treatment using first- and second-generation EGFR-TKIs compared to chemotherapy, 60% of patients developed resistance after the therapy due to the acquisition of the secondary point mutation T790M in exon 20 of the receptor [7]. Hence, a third-generation EGFR-TKI, osimertinib, was approved by the FDA in 2015 to treat patients whose tumors harbored a sensitizing mutation and/or T790M point mutation [8,9]. However, the acquisition of the secondary point mutation C797 in exon 20 led to patients developing resistance to osimertinib [10].

Apart from acquired secondary mutations in the EGFR gene, other resistance mechanisms have been described such as the activation of a signal transducer and activator of transcription 3 (STAT3) [11], c-Met amplification [12], IGF-1R activation [13], HER2 amplification [14], AXL activation [15], loss of PTEN expression, PIK3CA and BRAF mutations [16,17], and SCLC transformation [17]. Cancer stem cells (CSCs) are tumor-initiating cells resistant to radio- and chemotherapy that exhibit self-renewal and pluripotency capacities. This small proportion of tumor cells is responsible for relapse and metastasis [18,19]. Furthermore, CSCs have demonstrated clonogenic capacity and are able to grow in anchorage-independent in vitro conditions forming spheres [20].

Deregulation of cellular energy metabolism has been identified as a hallmark of cancer, and is fundamental for cell growth and division of cancer cells [21]. Fatty acid synthase (FASN) is a homodimeric and multi-functional enzyme responsible for *de novo* lipogenesis by catalyzing palmitate from acetyl CoA and malonyl CoA in a NADPH-dependent reaction [22]. It has been demonstrated that EGFRm mediates the resistance to EGFR-TKIs through the upregulation of the FASN expression [23], and consequently the inhibition of FASN resulted in cytotoxic effects on sensitive and EGFR-TKI-resistant EGFRm NSCLC cells [23,24]. Additionally, FASN inhibition caused the increase of radiosensitivity [25] and the reduction of cancer stem-like cells in NSCLC [26,27].

Therefore, the main objective of this study was to evaluate the novel FASN inhibitor, AZ12756122, both alone and in combination with gefitinib and osimertinib, in EGFRm lung adenocarcinoma cell models sensitive and resistant to EGFR-TKIs. Moreover, the molecular effect of AZ12756122 (again both alone and in combination with EGFR-TKI) was also analyzed on FASN, EGFR/STAT3, Akt/mTOR, and MAPK signaling pathways. The effect of the AZ12751622 compound against cancer stem-like cells was also explored. Furthermore, the FASN expression was evaluated in 36 tumor samples from patients with EGFRm NSCLC in order to validate in vitro results.

## 2. Material & methods

### 2.1. Chemicals & reagents

Roswell Park Memorial Institute (RPMI-1640) medium, L-glutamine 200 nM, phosphate-buffered saline (PBS), penicillin/streptomycin 10,000 U/mL, sodium pyruvate 100 nM, and trypsin 10 × were provided by Lonza (Basilea, Switzerland). Fetal bovine serum (FBS) and Dulbecco's Modified Eagle Medium (DMEM)/F12 (1:1) were obtained from HyClone (Logan, UT, USA). The bovine serum albumin (BSA) (≥98.0%), Bradford assay, crystal violet, lipoprotein-deficient FBS, paraformaldehyde, phenylmethylsulfonylfluoride (PMSF), TWEEN® 20, 3–(4,5–dimethyl-2–thiazolyl)-2,5–diphenyl-2 H-tetrazolium bromide (MTT), and primers (Supplementary Table 1) were acquired from Sigma-Aldrich (St. Louis, MO, USA). The BSA Fraction V pH for Western blotting (min. 96%) and tris-buffered saline (TBS) were purchased from PanReac AppliChem (Gatersleben, Germany). Ethanol absolute, dimethyl sulfoxide (DMSO), methanol, chloroform, sodium chloride, and potassium hydroxide were supplied by Labkem-Labbox Labware S. L. (Barcelona, Spain). Qiazol was provided from Qiagen (Hilden, Germany). The GeneJET RNA Purification Kit, West Femto Maximum Sensitivity Substrate, nitrocellulose membranes, and B-27™ supplement (50X) were obtained from Thermo Fisher Scientific Inc. (Waltham, MA, USA). The High-Capacity cDNA Archive Kit was acquired from Applied Biosystems (Foster City, CA, USA). The qPCRBIO SyGreen Mix Lo-Rox was purchased from PCR Biosystems Inc. (Wayne, PA, USA). DC Protein Assay, Clarity™ Western ECL Substrate, and 40% acrylamide solution were supplied by Bio-Rad (Hercules, CA, USA). The sample reducing agent and lithium dodecyl sulfate (LDS) sample buffer were provided by Invitrogen (Carlsbad, CA, USA) and the lysis buffer was obtained from Cell Signaling Technology (CST) Inc. (Danvers, MA, USA). Antibodies (Supplementary Table 1) were provided by CST, Abcam (Cambridge, UK), ProteinTech® (Manchester, UK), and Roche Diagnostics (Basilea, Switzerland). (1,2–14 C) acetic acid sodium salt was acquired from Perkin Elmer Biosciences (Waltham, MA, USA). Human epidermal growth factor (hEGF) 100 μg and human fibroblast growth factor (hFGF) 50 μg were purchased from Miltenyi Biotec (Bergisch Gladbach, Germany). The UltraView Universal DAB Detection Kit and Amplification Kit were supplied by Roche Diagnostics. The AZ12756122 compound, gefitinib, and osimertinib were kindly provided by AstraZeneca (London, UK).

### 2.2. Cell models

Human lung adenocarcinoma PC9 and its gefitinib-resistant (GR) derivative cell models PC9-GR1, PC9-GR3, and PC9-GR4 were kindly provided by Dr. R. Rosell and Dr. M.A. Molina (Barcelona, Spain). Mechanisms of resistance in GR models are indicated in Table 1. Cells were cultured in RPMI-1640 medium supplemented with 10% FBS and 50 U/mL penicillin/streptomycin and incubated at 37 °C in 5% $CO_2$ humidified environment and maintained mycoplasma-free.

### 2.3. Cell viability assay

Cells were seeded in adherent cell culture 96-well plates at the proper cell density. After 24 h, the cells were treated with a range of increasing concentrations of gefitinib, osimertinib, or AZ12756122 for 72 h for the monotreatment experiments. For the drug combination assay, cells were treated with three fixed concentrations of gefitinib (1, 2.5, and 5 μmol/L) or osimertinib (0.5, 1, and 2 μmol/L) in combination of different concentrations of AZ12756122 for 72 h. The MTT assay was employed to evaluate cell viability, as reported elsewhere [24]. Combinatorial effects were examined using the CompuSyn™ software (Biosoft, MO, USA) based on the Chou and Talalay approach [29]. The combination index (CI) value determines the effect of the drug combinations: $CI < 1$ designates a synergistic effect, $CI = 1$ designates an additive effect, and $CI > 1$ designates an antagonistic effect.

### 2.4. Fatty acid synthase activity assay

Cells were seeded in adherent cell culture 24-well plates at the appropriate cell density. After 24 h, the cells were treated with AZ12756122 at a concentration equivalent to their $IC_{50}$ or with the vehicle (DMSO) for 72 h and the medium was replaced by RPMI-1640 supplemented with 1% lipoprotein-deficient FBS. (1,2–$^{14}$C) acetic acid

**Table 1**
Mechanisms of resistance in gefitinib-resistant (GR) derivative PC9 cell models.

| Cell Model | T790M mutation | AXL overexpression | MET activation | EphA2 activation | Bcl-2 expression | FASN overexpression |
|---|---|---|---|---|---|---|
| PC9-GR1 | + | – | + | + | – | + |
| PC9-GR3 | – | + | – | – | + | + |
| PC9-GR4 | + | + | – | + | – | + |

*Source*: Modified from [28].

sodium salt (0.5 μCi/mL) was added to the medium for the last 6 h. The cell lysis and lipid extraction was accomplished as previously described [30]. Afterwards, cell pellets were radioactive-counted, and the Bradford assay was employed to quantify the total protein content.

### 2.5. Quantitative real-time PCR analysis

Cells were seeded in adherent cell culture plates at the proper cell density. After 24 h, the cells were treated with gefitinib, osimertinib or AZ12756122 at a concentration equivalent to their $IC_{50}$ as monotreatment or 25 μmol/L of AZ12756122 in combination with 1 μmol/L osimertinib for 72 h. Thereafter, the cells were rinsed with PBS and resuspended in 700 mL of Qiazol. RNA was isolated using a GeneJET RNA Purification Kit, quantified by a NanoDrop™ One Micro-volume UV–Vis spectrophotometer (Thermo Fisher Scientific, Waltham, MA, USA), and reverse-transcribed into complementary DNA (cDNA) employing a HighCapacity cDNA Archive Kit. Through the QuantStudio3 Real-Time PCR System (Thermo Fisher Scientific Inc., Waltham, MA, USA), different gene expression levels were determined using qPCRBIO SyGreen Mix Lo-Rox and primers (Table S1). The results were calculated using the standard formula $2^{\Delta CT}$ and normalized to the housekeeping GAPDH.

### 2.6. Western blotting analysis

Cells were seeded in adherent cell culture plates at the appropriate cell density. After 24 h, the cells were treated with gefitinib, osimertinib or AZ12756122 at a concentration equivalent to their $IC_{50}$ as monotreatment or 25 μmol/L AZ12756122 in combination with 1 μmol/L osimertinib for 72 h. Then, attached and floating cells were collected and lysed by vortexing every 5 min for 30 min in an ice-cold lysis buffer with 100 μg/mL PMFS. A DC Protein Assay was performed to obtain the protein concentration of each sample using a BSA standard curve. The same amounts of protein were heated in LDS and reducing agent buffers for 10 min at 70 °C, separated using SDS-polyacrylamide gel (SDS-PAGE) and moved to nitrocellulose membranes. Membranes were incubated for 1 h at room temperature in blocking buffer (5% skim milk powder in TBS 0.05% Tween (TBS-T)) and overnight at 4 °C with the corresponding primary antibody (Table S1) diluted in blocking buffer. Specific horseradish peroxidase (HRP)-conjugated secondary antibodies were incubated for 1 h at room temperature before being detected in the Bio-Rad ChemiDoc™ MP Imaging System (Bio-Rad Laboratories, Inc., Hercules, CA, USA) using an HRP substrate Clarity™ Western ECL Substrate or a West Femto Maximum Sensitivity Substrate.

### 2.7. Sphere formation assay

Cells were seeded in non-adherent cell culture 6-well plates at a low cell density for 7 days using DMEM/F12 medium supplemented with 20 ng/mL B27, hEGF, and hFGF, 1% L-glutamine, and 1% sodium pyruvate. The treatment with AZ12756122 at a concentration equivalent to their $IC_{10}$ and $IC_{30}$ was added at the moment of seeding. Thereafter, spheres bigger than 50 μm were counted using an inverted optical microscope. The Sphere Formation Index (SFI) was calculated using the following formula:

$$SFI = \frac{num.\ \ spheres}{num.\ \ cells\ \ seeded}$$

### 2.8. Colony formation assay

Cells were seeded in adherent cell culture 6-well plates at a low cell density for 7 days. The treatment with AZ12756122 at a concentration equivalent to their $IC_{10}$ and $IC_{30}$ was added at the moment of seeding. Afterwards, cells were rinsed with PBS and 2 mL of 6% paraformaldehyde + 0.5% of crystal violet was added to each well. After 30 min, the mixture was removed, the plates were washed by immersing them in tap water, and air-dried at room temperature. The Colony Formation Index (CFI) was calculated using the following formula:

$$CFI = \frac{num.\ \ colonies_{treatment}}{num.\ \ colonies_{control}}$$

### 2.9. Selection of patients

Between 2006 and 2019, forty-five patients from the Dr. Josep Trueta University Hospital (Girona, Spain) with NSCLC harboring exon 19 deletion and exon 21 L858R activating mutations in EGFR met the inclusion criteria. Tumor samples were obtained at the time of diagnostic biopsy prior to any treatment. The patients' clinical characteristics and pathological features of their tumors were examined retrospectively and obtained from their medical records. The Response Evaluation Criteria in Solid Tumors (RECIST) (version 1.1) was used to establish the response to the treatment (complete response, partial response, stable disease, and progression disease). All patients had received EGFR-TKI, gefitinib or erlotinib, at some point. It should be noted that some of patients in our study received other lines of treatment after receiving the EGFR-TKI. Thirty-six patients had sufficient tumor sample from their biopsies for immunohistochemical analysis.

### 2.10. Immunohistochemistry assay of tissue samples

BenchMark ULTRA-Ventana equipment (Roche Diagnostics) was employed to evaluate FASN tumor expression by immunohistochemistry (IHC) in 3 μm thick slides from formalin-fixed paraffin-embedded tissue blocks of the tumor. The FASN rabbit monoclonal antibody was detected using an UltraView Universal DAB Detection Kit and an Amplification Kit. Instead of the primary antibody, a similar concentration of mouse IgG was used as a negative control. Adipose tissue next to a FASN-overexpressing ductal-type breast carcinoma were also analyzed as a positive control for FASN expression. Negative FASN expression was deemed when none of the cells showed cytoplasmic staining. In contrast, any expression of FASN at the cytoplasmic level was classified as positive.

### 2.11. Data analysis

The statistical analysis was conducted using the IBM SPSS software (Version 25.0; SPSS Inc., Chicago, IL, USA) and R software (Version 4.0.4; The R Foundation, Vienna, Austria). The in vitro assays were replicated at least three times and the results expressed as mean ± standard error of the mean (SE). For two-group comparisons, non-parametric data were analyzed with the Mann–Whitney U test and

parametric data with the Student's t test. For the comparisons of more than two groups, non-parametric data were examined with the Kruskal–Wallis test and parametric data by one-way analysis of variance (ANOVA) using Bonferroni or Tamhane's T2 post hoc test. Data from patients were summarized as counts and percentages for categorical variables, and the number of non-missing observations, the mean ± standard deviation (SD), the median, or interquartile range [IQR] for continuous variables. Progression-free survival (PFS) probability was estimated according to the method of Kaplan–Meier and statistical differences were calculated using the log-rank test. Fisher's exact tests were employed to compare categorical variables. Levels of significance were determined at $p < 0.050$ and represented as follows: $p < 0.050$ (*), $p < 0.010$ (**), and $p < 0.001$ (***).

## 3. Results

### 3.1. Characterization of AZ12756122 compound

The cytotoxic effect of AZ12756122 was investigated through dose-response curves in lung adenocarcinoma cell models sensitive and resistant to EGFR-TKIs (Fig. 1A). The PC9-GR1 and PC9-GR4 cell models (T790M+) exhibit resistance exclusively to gefitinib, while the PC9-GR3 cell model (T790M-) is resistant to both gefitinib and osimertinib [28]. The half-maximal inhibitory concentration ($IC_{50}$) value of the compound was 64.3 ± 1.3 μM for PC9, 75.2 ± 6.4 μM for PC9-GR1, 45.7 ± 5.2 μM for PC9-GR3, and 76.8 ± 4.1 μM for PC9-GR4. Although no significant differences were found between the $IC_{50}$ value of PC9 and the GR models (PC9–GR1 $p = 1.000$; PC9–GR3 $p = 0.115$; PC9–GR4 $p = 0.756$), the $IC_{50}$ concentration of PC9-GR3 was significantly lower compared to the T790M+ models (PC9-GR1 $p = 9.960 \times 10^{-4}$; PC9-GR4 $p = 3.220 \times 10^{-4}$).

The ability of AZ12756122 to inhibit FASN activity was analyzed in sensitive and resistant models (Fig. 1B). The compound equally inhibited the enzyme activity in all cell models ($p = 0.566$), ranging from 38% to 54%, regardless of their sensitivity or resistance to EGFR-TKIs.

AZ12756122 treatment was also evaluated by Western blot to determine whether cell death was caused through the induction of apoptosis and/or autophagy in sensitive and GR models (Fig. 1C). The cleavage of poly (ADP-ribose) polymerase (PARP) and the conversion of the Light Chain 3 (LC3) into LC3-II were used as apoptosis and autophagy markers, respectively. The cleaved form of PARP (89 kDa) was observed in PC9, PC9-GR1, and PC9-GR3 following treatment with the compound, thus showing the induction of apoptosis. However, the LC3-II form did not appear, therefore the AZ12756122 treatment did not trigger autophagy.

### 3.2. Molecular effects caused by AZ12756122 and EGFR-TKIs treatments as single agents in EGFRm lung adenocarcinoma cell models

*FASN*, *EGFR*, and *STAT3* mRNA expression were analyzed after AZ12756122 or EGFR-TKIs treatment by means of RT-qPCR in cell models sensitive and resistant to EGFR-TKIs (Fig. 2). The mRNA expression of these genes was compared among cell lines and no significant differences were found. However, the EGFR levels trended to increase in the two T790M+ cell models, whereas the STAT3 expression trended to decrease, especially in PC9-GR3 and PC9-GR4 cells (Supplementary Fig. 1).

While the AZ12756122 treatment reduced *FASN* mRNA levels in all models, it was statistically significant in PC9 ($p = 5.5 \times 10^{-4}$), PC9-GR1 ($p = 0.009$), and PC9-GR4 ($p = 0.049$) compared to the control. Furthermore, gefitinib and osimertinib treatments also diminished the *FASN* mRNA expression in the T790M- models (PC9 ($p = 4.5 \times 10^{-4}$)

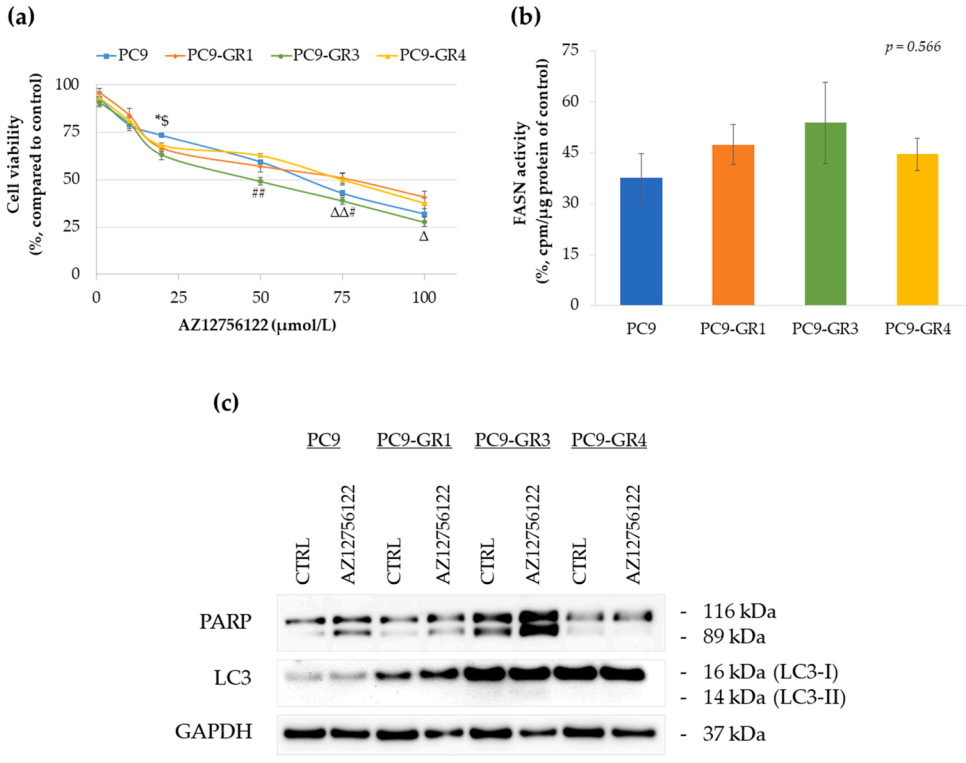


**Fig. 1.** (a) Dose-response curves of AZ12756122 compound in sensitive and gefitinib-resistant (GR) models. Sensitive (PC9) and GR models (PC9-GR1, PC9-GR3, and PC9-GR4) were treated with increasing concentrations of AZ12756122 (from 1 to 100 μmol/L) for 72 h. Results shown are expressed as percentage of surviving cells after drug treatment (mean ± SE) from at least three independent experiments. * $p < 0.050$, ** $p < 0.010$, and *** $p < 0.001$ indicate levels of statistical significance. The symbol * indicates differences between PC9 and PC9-GR1, $ indicates differences between PC9 and PC9-GR3, # indicates differences between PC9-GR3 and PC9-GR4, and Δ indicates differences between PC9-GR1 and PC9-GR3. (b) AZ12756122 compound inhibits FASN activity in sensitive and GR models. PC9 and GR models were treated with AZ12756122 at a concentration equivalent to their $IC_{50}$ and with DMSO as the control for 72 h. FASN activity was assayed by counting radiolabeled fatty acids synthesized *de novo*. Results shown are the percentage of remaining activity (mean ± SE) in treated versus untreated cells (control) from at least three independent experiments. (c) Effect of AZ12756122 on apoptosis and autophagy determined by PARP cleavage and LC3 conversion in sensitive and GR models. PC9 and GR models were treated with the AZ12756122 compound at a concentration equal to their $IC_{50}$ for 72 h. Untreated cells were used as an internal control (CTRL), and GAPDH as a loading control. Results shown are representative from at least three independent experiments.

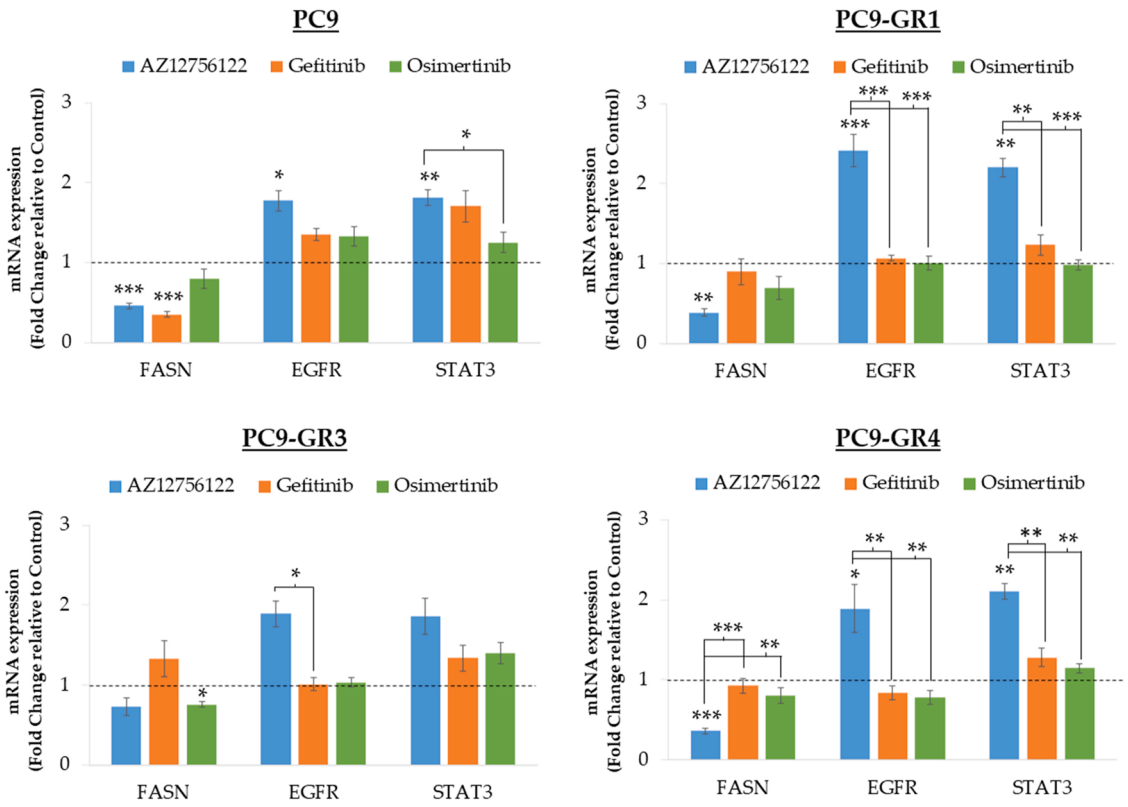


**Fig. 2.** *FASN*, *EGFR*, and *STAT3* mRNA expression after AZ12756122 and EGFR-TKIs (gefitinib and osimertinib) treatments in sensitive and gefitinib-resistant (GR) models. Sensitive (PC9) and GR models (PC9-GR1, PC9-GR3, and PC9-GR4) were treated with AZ12756122, gefitinib or osimertinib at a concentration equivalent to their $IC_{50}$ for 72 h. mRNA levels were obtained by RT-qPCR and normalized against the GAPDH gene. All conditions were compared to the control (untreated cells), which was normalized to 1 (indicated by the dotted line) and expressed as a fold change. Experiments were performed at least three times. * $p < 0.050$, ** $p < 0.010$, and *** $p < 0.001$ indicate levels of statistically significance.

and PC9-GR3 ($p = 0.046$), respectively), compared to control. An increase in *EGFR* mRNA levels was observed in the AZ12756122 treatment, which was statistically significant in PC9 ($p = 0.021$), PC9-GR1 ($p = 6.0 \times 10^{-6}$), and PC9-GR4 ($p = 0.014$) compared to control and also in comparison with the gefitinib treatment in the GR models (PC9-GR1 $p = 1.0 \times 10^{-5}$; PC9-GR3 $p = 0.036$; PC9-GR4 $p = 0.004$) and with the osimertinib treatment in the T790M+ cell models (PC9-GR1 $p = 6.0 \times 10^{-6}$; PC9-GR4 $p = 0.003$). The AZ12756122 treatment also upregulated the *STAT3* mRNA expression in all models, and was statistically significant in PC9 ($p = 0.006$), PC9-GR1 ($p = 0.003$), and PC9-GR4 ($p = 0.009$) compared to control and also in comparison with the gefitinib treatment in the T790M+ cell models (PC9-GR1 $p = 0.003$; PC9-GR4 $p = 0.009$) and with the osimertinib treatment (PC9 $p = 0.049$; PC9-GR1 $p = 3.5 \times 10^{-4}$; PC9-GR4 $p = 0.002$). Additionally, an increase of *STAT3* was also shown in the gefitinib treatment in the sensitive model.

Alterations in protein expression caused by AZ12756122, gefitinib and osimertinib were also evaluated in both sensitive and GR models (Fig. 3).

The FASN protein expression was decreased by the AZ12756122 treatment in all cell models. Moreover, the treatment using the compound or EGFR-TKIs reduced phosphorylated levels of EGFR in both the sensitive and GR models. The osimertinib treatment activated STAT3 levels, whereas AZ12756122 did not cause variations in the GR cell models. The gefitinib treatment also increased the phosphorylated levels of STAT3 in all models. No alterations were showed in the STAT3 total protein expression. Moreover, no changes were found in MAPK signaling pathway activation or expression. Focusing on the Akt/PRAS40 signaling pathway, the treatment using the compound reduced the activation of Akt in the GR models and PRAS40 in all cell models. Furthermore, the AZ12756122 treatment slightly decreased PRAS40 total protein expression. Although the gefitinib treatment reduced Akt and PRAS40 total protein levels in PC9, their phosphorylated levels were higher than untreated cells. The osimertinib treatment diminished the activation of Akt in all cell models and PRAS40 in PC9 and PC9-GR1.

### 3.3. Pharmacological interaction between AZ12756122 and EGFR-TKIs

The combinatorial treatment using AZ12756122 and EGFR-TKIs was studied to find synergistic interactions and overcome the acquired resistance to gefitinib in the T790M+ models, PC9-GR1 and PC9-GR4, and to gefitinib and osimertinib in the T790M- model, and PC9-GR3 (Fig. 4). Furthermore, $IC_{50}$ values of all combinatorial treatments were calculated (Supplementary Table 2).

None of the combinations tested showed synergism in PC9-GR1. The different combinatorial treatments resulted in an antagonism or additive effect. The AZ12756122 $IC_{50}$ value significantly decreased in combination with 2.5 μM gefitinib ($p = 0.037$) and 5 μM gefitinib ($p = 1.0 \times 10^{-5}$) in comparison with the AZ12756122 monotreatment and other combinations (AZ12756122 + 1 μM gefitinib $p = 2.2 \times 10^{-4}$; AZ12756122 + 2.5 μM gefitinib $p = 0.019$).

In the PC9-GR4 cell model, some combinations exhibited synergistic effects. It should be highlighted that the highest concentration of gefitinib (5 μM) was required with lower concentrations of AZ12756122 to obtain a synergistic effect, and vice versa. The combination of AZ12756122 + 5 μM gefitinib was the only one that showed a significantly lower $IC_{50}$ value compared to monotherapy ($p = 5.7 \times 10^{-9}$) and to the other combinations (AZ12756122 + 1 μM gefitinib $p = 4.8 \times 10^{-7}$; AZ12756122 + 2.5 μM gefitinib $p = 3.0 \times 10^{-6}$).

Regarding the T790M- GR model, the combination using gefitinib

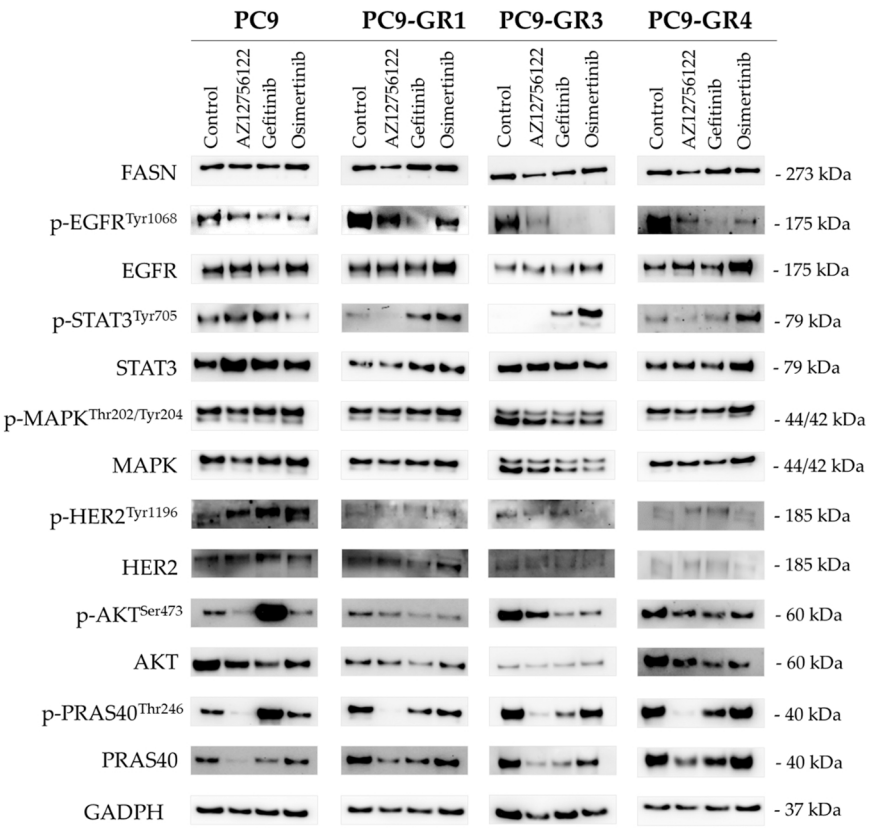


**Fig. 3.** Analysis of protein expression after treatment using AZ12756122 and EGFR-TKIs (gefitinib and osimertinib) in sensitive and gefitinib-resistant (GR) models. Sensitive (PC9) and GR models (PC9-GR1, PC9-GR3, and PC9-GR4) were treated with AZ12756122, gefitinib or osimertinib at a concentration equal to their $IC_{50}$ for 72 h. Untreated cells were used as an internal control (CTRL) and GAPDH as a loading control. Results shown are representative of at least three independent experiments.

demonstrated mostly additive and synergistic effects. Nevertheless, combinations with synergistic effects were obtained at higher concentrations. No significant differences were found between the $IC_{50}$ value of AZ12756122 monotherapy and combinatorial treatments or among combination curves. The combination of AZ12756122 and osimertinib exhibited only additive or synergistic effects. Unlike the combinatorial treatments using gefitinib, the combination with the lowest concentrations showing synergistic effects (25 μM AZ12756122 + 1 μM osimertinib) also demonstrated a cell viability above 50%. Additionally, the $IC_{50}$ value diminished with increasing osimertinib concentrations, and was significantly lower in the combination of AZ12756122 + 1 μM osimertinib in comparison with monotreatment ($p = 0.003$),

and the combination AZ12756122 + 2 μM osimertinib, in contrast to monotherapy ($p = 3.9 \times 10^{-5}$) and other combinations (AZ12756122 + 0.5 μM osimertinib $p = 0.002$; AZ12756122 + 1 μM osimertinib $p = 0.016$).

Therefore, the effects of the combinatorial treatment of 25 μM AZ12756122 and 1 μM osimertinib on mRNA and protein expression were studied in the PC9-GR3 cell model (Fig. 5).

In terms of mRNA expression, no changes were observed in the FASN expression for monotherapies or combinatorial treatment. The EGFR expression was significantly enhanced by AZ12756122 monotreatment compared to untreated cells ($p = 0.022$). Moreover, AZ12756122 monotherapy and its combination with osimertinib demonstrated increased EGFR expression in comparison with osimertinib monotherapy (AZ12756122 $p = 0.004$; AZ12756122 + osimertinib $p = 0.041$). Although the STAT3 expression did not show significant variations as a result of the monotreatments, the combinatorial therapy upregulated its expression compared to untreated cells and osimertinib monotreatment (control $p = 0.012$; osimertinib $p = 0.014$).

The FASN protein expression was only slightly decreased in the AZ12756122 monotreatment. All treatments caused a reduction in EGFR activation, and furthermore AZ12756122 monotreatment slightly diminished total EGFR expression. Although no changes in total STAT3 levels were observed, both osimertinib monotherapy and combinatorial treatment showed high levels of phosphorylated STAT3 compared to untreated cells. Both AZ12756122 monotherapy and combinatorial treatment decreased MAPK activation and total expression, whereas osimertinib monotherapy increased its phosphorylated levels. Regarding Akt/mTOR signaling pathways, although AZ12756122 monotreatment reduced total Akt expression, osimertinib monotherapy and combinational treatment decreased its activation. The activation of PRAS40 was diminished in both monotreatments and combinatorial therapy, but total PRAS40 protein levels were only reduced in AZ12756122 monotreatment and combinatorial therapy.

### 3.4. AZ12756122 activity against cancer stem-like population

AZ12756122 activity against cancer stem-like cells was evaluated using sphere and colony formation assays in sensitive and gefitinib- and osimertinib-resistant cell models (Fig. 6).

AZ12756122 treatment, using its $IC_{10}$ concentration, resulted in a significant reduction of spheres ($p = 0.023$) and colonies ($p = 9.7 \times 10–5$) in PC9 cells and of spheres in PC9-GR3 cells ($p = 0.009$). No changes in colony formation were found in PC9-GR3 cells. Furthermore, the $IC_{30}$ concentration treatment exhibited a significant decrease in spheres (PC9-GR3, $p = 0.008$) and colonies (PC9, $p = 2.0 \times 10–6$; PC9-GR3, $p = 2.5 \times 10–5$) in contrast to untreated cells and the treatment using $IC_{10}$ concentration (colonies PC9, $p = 1.3 \times 10–4$; spheres PC9-GR3, $p = 0.009$; colonies PC9-GR3, $p = 9.0 \times 10–5$). Total inhibition of sphere formation was observed in PC9 cells.

### 3.5. FASN expression in EGFRm NSCLC patients

Data were collected from forty-five NSCLC patients harboring exon 19 deletion or exon 21 L858R sensitizing mutations (Table 2). Data for FASN expression levels were also collected (Supplementary Table 3).

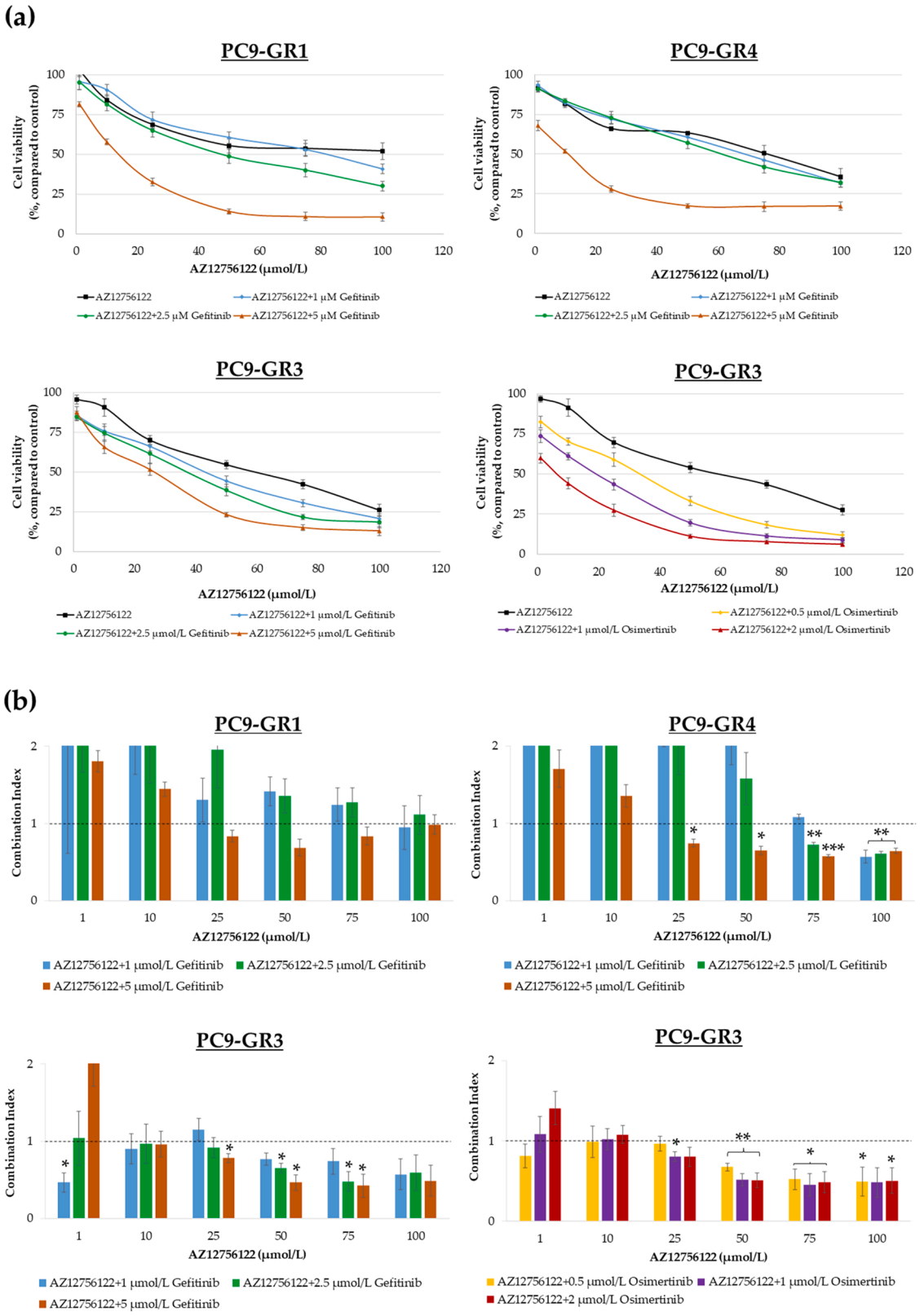


**Fig. 4.** Combinatorial treatment between AZ12756122 and EGFR-TKIs (gefitinib and osimertinib) in gefitinib-resistant (GR) models. (a) Dose-response curves of AZ12756122 (from 1 to 100 μM) alone and in combination with gefitinib (1, 2.5 and 5 μM) in PC9-GR1, PC9-GR3, and PC9-GR4 models and osimertinib (0.5, 1 and 2 μM) in PC9-GR3 for 72 h. Results shown are expressed as percentage of surviving cells after drug treatment (mean ± SE) from at least three independent experiments. (b) Combination Index (CI) from treatments with AZ12756122 (from 1 to 100 μM) and gefitinib (1, 2.5 and 5 μM) in PC9-GR1, PC9-GR3, and PC9-GR4 models or osimertinib (0.5, 1 and 2 μM) in PC9-GR3 for 72 h. Results shown are mean ± SE from at least three independent experiments and are based on the Chou and Talalay method. The dotted line indicates additive (CI approximately equal to 1). CI > 1 designates antagonistic effect and CI < 1 synergistic effect * $p < 0.050$, ** $p < 0.01$, *** $p < 0.001$ indicate levels of statistical significance.

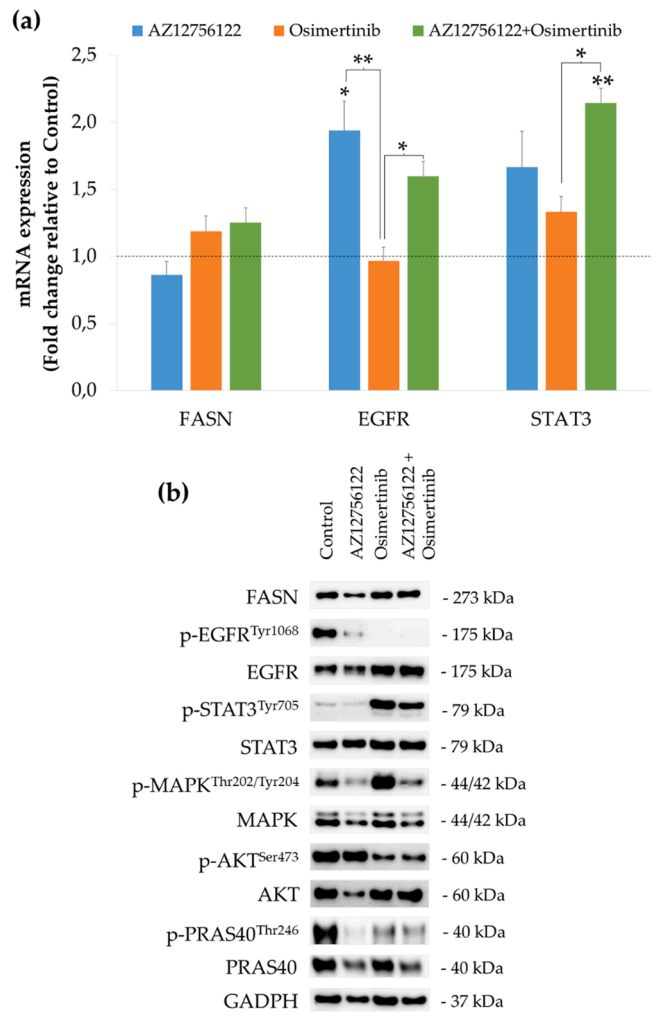


**Fig. 5.** Effects on mRNA levels and protein expression caused by the combination treatment in the PC9-GR3 cell model. (a) FASN, EGFR, and STAT3 mRNA expression levels after the combination treatment. PC9-GR3 models were treated with 25 μM AZ12756122, 1 μM osimertinib or both treatments for 72 h. mRNA levels were obtained by RT-qPCR and normalized against the GAPDH gene. All conditions were compared to the control (untreated cells), which was normalized to 1 (indicated by the dotted line) and expressed as a fold change. Experiments were performed at least three times. * $p < 0.050$, ** $p < 0.010$, and *** $p < 0.001$ indicate levels of statistical significance. The symbol * indicates in comparison with control, $ indicates in comparison with AZ12756122 treatment, and # indicates in comparison with osimertinib treatment. (b) Protein expression after the combination treatment. PC9-GR3 models were treated with 25 μM of AZ12756122, 1 μM of osimertinib or both treatments for 72 h. Untreated cells were used as an internal control (CTRL) and GAPDH as a loading control. Results shown are representative of at least three independent experiments.

FASN tumor expression was analyzed in thirty-six biopsies with sufficient tumor sample for immunohistochemical (IHC) evaluation (Fig. 7). A positive expression of FASN was observed in seventeen (47.2%) of the tumor samples. Median progression-free survival (mPFS) was significantly longer in patients whose tumors expressed some levels of FASN at baseline ($p = 0.039$) (Fig. 7A). PFS refers to the time from the onset of treatment to the occurrence of disease progression or death. The expression of FASN also trend to a better response rate to the EGFR-TKI ($p = 0.060$) (Supplementary Fig. 2B). Furthermore, mPFS was analyzed according to the response to the EGFR-TKI treatment and FASN expression. Patients who responded to EGFR-TKI treatment and who expressed FASN showed significantly longer mPFS than those who did not express FASN ($p = 0.015$) (Fig. 7 B). However, no relationship between FASN tumor expression and overall survival (OS) was detected ($p = 0.490$) (Supplementary Fig. 2A). OS refers to the time elapsing from the beginning of treatment to death for any reason.

## 4. Discussion

Although different EGFR-TKIs have been approved for the treatment of EGFRm NSCLC patients [5,9], several mechanisms have been described by which cells acquire resistance, such as FASN overexpression [23,24] or the increase of CSCs [18,19]. Previous studies have showed that FASN inhibition caused cytotoxic effects in EGFRm lung adenocarcinoma [23,24] and reduced cancer stem-like cells in NSCLC [26,27]. Therefore, this study evaluated the effect of a novel FASN inhibitor, AZ12756122, both alone and in combination with EGFR-TKIs, in cell models sensitive and resistant to EGFR-TKIs, and in their cancer stem-like cell populations. Furthermore, the FASN expression was analyzed in EGFRm NSCLC patients to validate the in vitro results.

The AZ12756122 compound inhibited FASN activity in both sensitive and resistant to EGFR-TKIs cell models (Fig. 1B). Other compounds inhibited FASN activity [24,31], such as Orlistat, an FDA-approved anti-obesity drug, which reduced FASN activity in H1975 cells, but not in PC14 and H3255 cells [31]. Additionally, it was previously observed that FASN knockdown inhibited cell proliferation [32] inducing apoptosis through the increase of the autophagosomal marker LC3-II [33]. However, only apoptosis induction was observed in PC9, PC9-GR1, and PC9-GR3 (Fig. 1C). Despite that, AZ12756122 exhibited cytotoxic effects in all cell models tested (Fig. 1A), suggesting that AZ12756122 treatment only affected cell growth in PC9-GR4. AZ12756122 $IC_{50}$ values oscillated from 45 to 77 μM, lower concentrations than those used with (−)-epigallocatechin-3–gallate (EGCG) or Orlistat [23,24]. PC9-GR3 cells were significantly more sensitive to the AZ12756122 treatment than the T790M+ cell models were. These results may be due to the activation of EphA2 exhibited by the T790M+ models [28]. Youngblood et al., demonstrated that EphA2 overexpression led to increased lipogenesis and tumor growth in breast cancer cells [34]. Other FASN inhibitors also reduce the cell viability of cisplatin-resistant cells [27] and induced apoptosis in NSCLC cells [26].

GR EGFRm NSCLC cells exhibited overexpression of FASN [23,24]. Despite this, the AZ12756122 treatment decreased FASN mRNA and protein expression in all cell models (Figs. 2 and 3). This may influence the lipid content of cell membranes, since the main product of FASN is palmitate, from which different fatty acids can be formed. Moreover, the sterol regulatory element binding protein (SREBP)− 1 is a master regulator of FASN and its ablation induces the apoptosis of cancer cells [35,36]. Phosphorylated EGFR levels were also diminished in all cell models (Figs. 2 and 3). Previous findings revealed that FASN inhibition also reduced FASN and EGFR protein expression in GR EGFRm NSCLC [23] and EGFRwt NSCLC [37]. Nonetheless, our research group and other researchers proved that the inhibition of FASN activity did not affect EGFR activation or its expression [24], nor did it affect FASN protein levels [24,38]. All together this suggests that although EGFR is involved in FASN regulation [23,39], the inhibition of FASN activity may not directly affect EGFR. Regarding Akt/mTOR signaling pathway, AZ12756122 reduced phosphorylated levels of Akt and PRAS40 in all cell models (Fig. 3), irrespective of their resistance to EGFR-TKIs. These results are in line with previous research [26,32,39,40]. Hence, EGFR may be another AZ12756122-direct target. The compound inhibited the Akt/PRAS40 pathway resulting in lower levels of sterol response element-binding proteins 1c (SREBP-1c) [35] and/or downstream effectors such as S6K [41] and, consequently, in FASN downregulation.

The sustained STAT3 activation found after the EGFR-TKI treatment is consistent with the literature [42]. STAT3 remained inactive after the AZ12756122 treatment in the GR models (Fig. 3). Similar results have been observed with other FASN inhibitors in EGFRm NSCLC [24], head and neck carcinomas [43], and pancreatic cancer [44]. Previously,

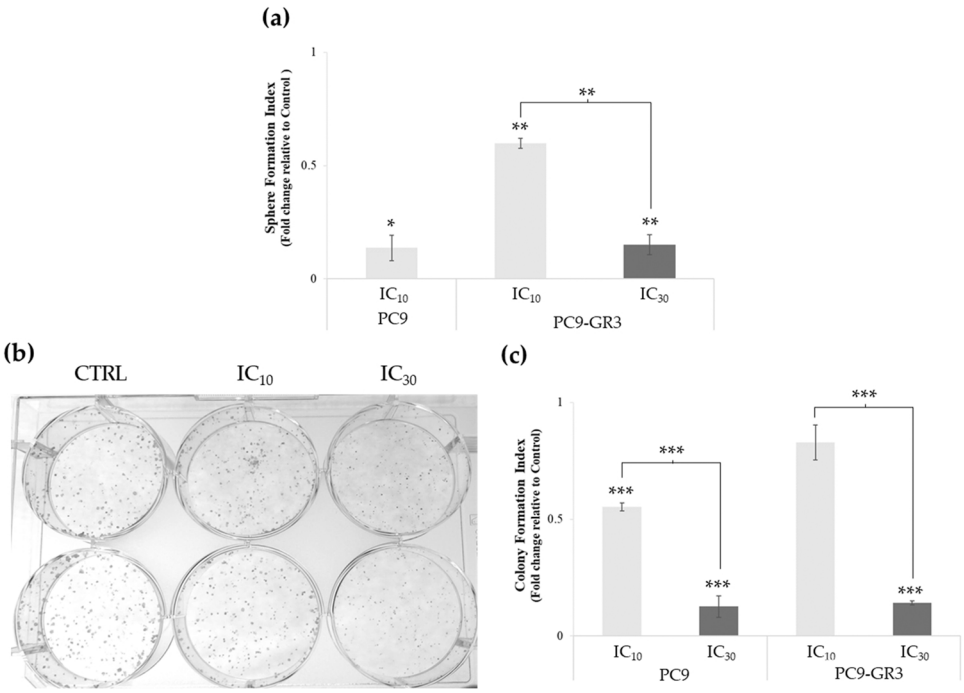


**Fig. 6.** AZ12756122 activity against cancer stem-like cells in sensitive and gefitinib-resistant (GR) models. (a) Sphere formation after AZ12756122 treatment. Cells were treated at concentrations equivalent to their $IC_{10}$ and $IC_{30}$ for 7 days. All conditions were compared to the control (untreated cells), which was normalized to 1 and expressed as a fold change. (b) Colony formation assay (c) Colony formation after AZ12756122 treatment. Cells were treated at concentrations equivalent to their $IC_{10}$ and $IC_{30}$ for 7 days. All conditions were compared to the control (untreated cells), which was normalized to 1 and expressed as a fold change. Experiments were performed at least three times. Statistical differences are indicated as * $p < 0.05$, ** $p < 0.01$ and *** $p < 0.001$.

**Table 2**
Patient and tumor characteristics at baseline.

| | Number | Percentage |
|---|---|---|
| **Gender** | | |
| Female | 34 | 75.6 |
| Male | 11 | 24.4 |
| **Age (Years)** | | |
| Median (Q1;Q3) | 68 | 58;74 |
| Min; Max | 46;88 | |
| **Smoking Habit** | | |
| Never | 33 | 73.3 |
| Former | 8 | 17.8 |
| Current | 4 | 8.9 |
| **ECOG** | | |
| 0 | 15 | 33.3 |
| 1 | 26 | 57.8 |
| 2 | 4 | 8.9 |
| **Histology** | | |
| Adenocarcinoma | 41 | 91.2 |
| Adenosquamous | 2 | 4.4 |
| Squamous | 2 | 4.4 |
| **EGFR Mutation** | | |
| Exon 19 | 26 | 57.8 |
| Exon 21 | 19 | 42.2 |
| **Response Rate to TKI** | | |
| Complete Response | 1 | 2.2 |
| Partial Response | 30 | 66.7 |
| Stable Disease | 7 | 15.6 |
| Progression Disease | 6 | 13.3 |
| Missing | 1 | 2.2 |
| **FASN Expression** | | |
| Negative | 19 | 42.2 |
| Positive | 17 | 37.8 |
| Missing | 9 | 20.0 |
| **EGFR-TKI Treatment Line** | | |
| First Line | 37 | 82.2 |
| Second Line | 8 | 17.8 |

inhibition of the MAPK pathway was exhibited after treatments using FASN inhibitors or EGFR-TKIs in lung cancer [28,32,39]; which disagrees with our findings from the sensitive and T790M+ cell models. However, Geng et al. proved that the constant activation of MAPK pathway caused by a FASN inhibitor resulted in the induction of apoptosis by upregulating apoptosis-related proteins and down-regulating pro-survival ones [45].

A combination of therapies is a widely-studied strategy to overcome EGFR-TKI resistance [32]. Palmitate overproduction has been linked to alterations in cellular response to anticancer drugs [46] and the survival of EGFR-TKI resistant EGFRm NSCLC cells [23]. Our findings show that the combinatorial treatment of AZ12756122 and gefitinib had mostly additive effects (Fig. 4). Only PC9-GR3 and PC9-GR4 cell models exhibited synergistic effects in some combinations. These results could be related to the inability of gefitinib to inhibit the Akt/mTOR signaling pathway in PC9-GR1 cells (Fig. 3), most likely due to the MET activation observed in this cell model [28]. Moreover, the Akt/mTOR signaling pathway has been proven to play an essential role in the survival of GR EGFRm NSCLC cells [23]. In PC9-GR3, the combination of AZ12756122 and osimertinib demonstrated synergistic effects and inhibition EGFR, Akt, PRAS40, and MAPK activation compared to untreated cells (Figs. 4 and 5). However, the combinatorial treatment did not prevent the STAT3 activation caused by osimertinib, which is consistent with the literature [24]. Previous studies have also found synergistic effects using the combinatorial treatment of EGFR-TKIs and Akt [28] and MAPK [47] inhibitors in EGFR-TKI-resistant NSCLC cells. Jacobsen et al., proved that Akt and MAPK activation persisted in resistant cells treated using EGFR-TKI and Akt inhibitors [28]. Akt/mTOR and MAPK signaling pathway activation is directly related to the activation and over-expression of FASN [48]. All together this suggests that FASN inhibition may be a better strategy to reduce the activation of these signaling pathways which play a key role in EGFR-TKI resistance.

The treatment using the AZ12756122 compound showed a reduction of CSC population PC9 and PC9-GR3 (Fig. 6). This subpopulation is related to resistance, relapse, and metastasis [18,19]. Similar findings were exhibited in breast cancer [49–51] and colorectal cancer [52,53]. In NSCLC, FASN inhibition has been demonstrated to cause a decrease of clonogenicity [26], migration and invasion capacities [32]. As shown in Fig. 3, AZ12756122 also caused the inhibition of Akt and PRAS40. Different studies have demonstrated that the Akt/mTOR signaling pathway is directly related to the CSC niche [50,54]. All together this suggests that FASN inhibition may reduce the CSC population by inhibiting the Akt/mTOR signaling pathway.

The demographic characteristics of our population with NSCLC

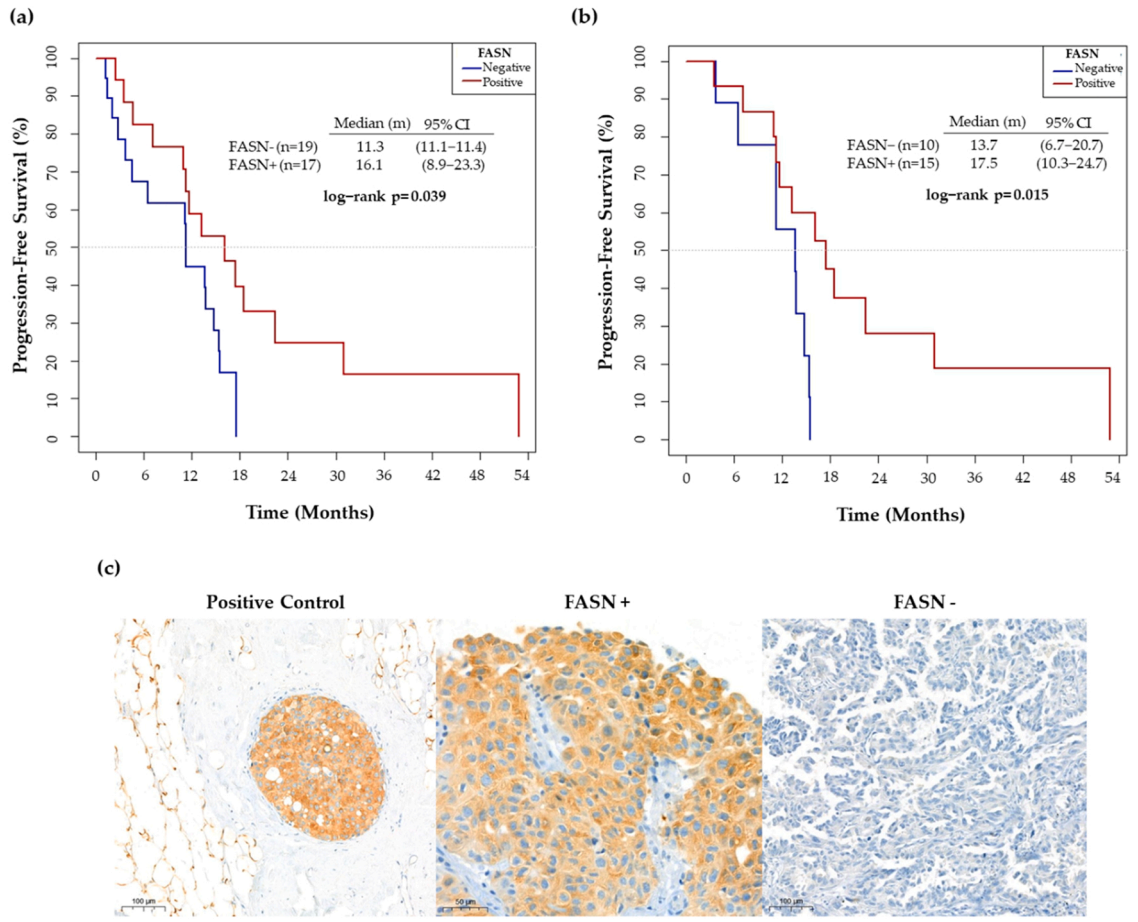


**Fig. 7.** (a) Median progression-free survival according to the immunohistochemistry (IHC) expression levels of FASN. The non-expression of FASN was considered as negative and any expression of FASN as positive. (b) Median progression-free survival in EGFR-TKI responders (complete response + partial response) according to the IHC expression levels of FASN. The non-expression of FASN was considered as negative and any expression of FASN as positive. (c) IHC staining of FASN in paraffin-embedded core biopsies from NSCLC patients harboring sensitizing mutations in the EGFR gene.

harboring EGFR sensitive mutations are consistent with those published in large European studies [55]. To the best of our knowledge, this is the first study to report standard levels of FASN expression in EGFRm NSCLC patients. Previous studies observed that FASN expression was higher in tumor tissues than normal and adjacent tissues [33,38,56]. FASN expression was found in 47.2% of tumor samples. Other researchers have observed FASN expression in lung adenocarcinoma samples ranging from 22% to 81% [38,57,58]. However, mutations in the EGFR gene or in other oncogenes were not considered in these investigations. No relationship was found between FASN expression and overall survival in our population, which is in agreement with the literature [38,57,59]. Additionally, FASN expression was significantly associated with longer mPFS, longer mPFS in patients who responded to EGFR-TKI treatment, and trends to a better response to the EGFR-TKI (Fig. 7), suggesting that FASN expression at baseline may have a role in a better outcome in patients with NSCLC harboring EGFR sensitizing mutations. In fact, our study (Fig. 3) and other authors [23] have demonstrated that the gefitinib treatment diminished mRNA and protein expression of FASN only in PC9 cells, i.e., the sensitive cell model. Researchers have also reported that: [1] EGFRm regulates the expression of FASN to palmitoylate EGFR and localizes it into the cell membrane of PC9 cells [23,60], and [2] FASN inhibition results in EGFR ubiquitination [23]. Taken all together, our hypothesis is that the mPFS, the response to EGFR-TKI treatment, and the mPFS according to the response to the EGFR-TKI treatment, were better in tumor samples from biopsies of FASN+ EGFRm NSCLC patients because the EGFR-TKI therapy had a dual effect: downregulating the FASN expression and inhibiting EGFR activation. Nevertheless, our study had some methodological limitations that may have influenced the results. First, it was retrospective research, with the biases that involves. Second, the number of samples with sufficient tissue to perform IHC was lower than expected. Third, some tumor samples were relatively old, which may have influenced the IHC results. Nonetheless, in this regard, the percentage of FASN expression detected in our samples is comparable to that observed in previous studies.

## 5. Conclusions

Inhibition of FASN activity is a promising strategy for treating EGFRm NSCLC. The novel FASN inhibitor AZ12756122 downregulated FASN expression and activity, caused cytotoxic effects, and induced apoptosis in sensitive and EGFR-TKI-resistant EGFRm NSCLC cells. The compound also reduced phosphorylated levels of EGFR and Akt/PRAS40. Furthermore, the combinatorial treatment of AZ12756122 and osimertinib overcame resistance to EGFR-TKI, exhibiting a synergistic effect which resulted in a decrease of EGFR, Akt/PRAS40, and MAPK activation. AZ12756122 also showed activity against cancer stem-like cells in both sensitive and gefitinib- and osimertinib-resistant cell models. Finally, our study revealed that FASN+ EGFRm NSCLC patients who responded to EGFR-TKI treatment exhibited a significantly longer mPFS than those who did not express FASN. Therefore, these findings suggest that FASN inhibition should be studied further in the treatment, alone or in combination with EGFR-TKIs, of EGFRm NSCLC patients.

## Funding

This research was funded by AstraZeneca (NCR-18-13804). The funders had no role in the design of the study, in the collection, analyses, or interpretation of data, in the writing of the manuscript, or in the decision to publish the results.

## CRediT authorship contribution statement

**EPA, RP, SRM, JC, and TP**: Conceptualization. **EPA, JR, and CVD**: Methodology. **EPA, SRM, CVD, JR, RP, and JBB**: Validation. **EPA, RP and JBB**: Formal analysis. **EPA, JR, RP, and CVD**: Investigation. **JC, TP, RP, and JBB**: Resources. **EPA, RP and JBB**: Data curation. **EPA and RP**: Writing – original draft. **EPA, RP, SRM, and JBB**: Writing – review & editing. **EPA**: Visualization. **JC, TP**: Supervision. **JC, TP, RP, and JBB**: Project administration. **JC and TP**: Funding acquisition. All authors have read and agreed to the published version of the manuscript.

## Conflict of interest statement

The authors declare the following financial interests/personal relationships which may be considered as potential competing interests: Teresa Puig reports financial support was provided by AstraZeneca. Joaquim Bosch-Barrera reports a relationship with Roche-Genentech that includes: funding grants. Joaquim Bosch-Barrera reports a relationship with Pfizer that includes: funding grants. Joaquim Bosch-Barrera reports a relationship with MSD Spain that includes: funding grants. Joaquim Bosch-Barrera reports a relationship with BMS that includes: funding grants. Joaquim Bosch-Barrera reports a relationship with AstraZeneca that includes: funding grants. Joaquim Bosch-Barrera reports a relationship with Novartis that includes: funding grants. Joaquim Bosch-Barrera reports a relationship with Boehringer-Ingelheim that includes: funding grants and travel reimbursement. Joaquim Bosch-Barrera reports a relationship with Vifor that includes: funding grants. Joaquim Bosch-Barrera reports a relationship with Sanofi that includes: funding grants. Joaquim Bosch-Barrera reports a relationship with LEO Pharma that includes: funding grants. Rut Porta reports a relationship with Pfizer that includes: funding grants. Rut Porta reports a relationship with Rovi that includes: funding grants. Rut Porta reports a relationship with Sanofi that includes: funding grants. Dra. Porta reports personal fees from Pfizer, Rovi, and Sanofi, outside the submitted work. Dr. Bosch-Barrera reports grants and personal fees from Roche-Genentech and Pfizer, and personal fees from MSD, BMS, AstraZeneca, Novartis, Boehringer-Ingelheim, Vifor, Sanofi, and LEO Pharma, outside the submitted work. The other authors declare that they have no competing interests.

## Acknowledgments

The authors acknowledge the pre-doctoral grant of E.P.A. (2019FI_B01011), and the post-doctoral grant of S.R.M. (POST-DOCUDG-2020–0002), as well as the support of the Catalan Government (2017SGR00385), the Oncolliga Foundation and RadikalSwim (OncoSwim). The authors are grateful to R. Rosell and M. A. Molina from the laboratory of Oncology Pangaea (Barcelona, Spain) for kindly providing PC9 models. The authors would particularly like to acknowledge the patients and the IDIBGI Biobank for their collaboration. The authors are also grateful to the pharmacist Maria López and the Clinical Trial Unit of Catalan Institute of Oncology for the help provided in identifying the patients treated with EGFR-TKI. The authors also thank Maria Buxó for her statistical analysis support of patients' samples. The authors also acknowledge Glòria Oliveres for the help provided in sample identification and management.

### *Institutional Review Board Statement*

Samples from patients included in this study were processed following standard operating procedures with the appropriate approval from the Ethics and Scientific Committees. Approval of the study protocol was obtained from the Dr. Josep Trueta University Hospital Clinical Research Ethics Committee (CP_FASN_T790M_2017; approved 1 June 2017).

### *Informed Consent Statement*

Samples from patients included in this study were provided by the Girona Biomedical Research Institute (IDIBGI) Biobank (Biobanc IDIBGI, B.0000872), integrated into the Spanish National Biobanks Network and in the Xarxa de Bancs de Tumors de Catalunya (XBTC) financed by the Pla Director d'Oncologia de Catalunya. All patients consented to the storage of the samples in the biobank and for their use in research projects.

### *Data availability*

All data generated or analyzed during this study are included in this published article [and its supplementary information files].

## Appendix A. Supporting information

Supplementary data associated with this article can be found in the online version at doi:10.1016/j.biopha.2022.113942.

## References

[1] H. Sung, J. Ferlay, R.L. Siegel, M. Laversanne, I. Soerjomataram, A. Jemal, et al., Global Cancer Statistics 2020: GLOBOCAN estimates of incidence and mortality worldwide for 36 cancers in 185 countries, CA Cancer J. Clin. (3) (2021) 209–249.
[2] M.L. Forsythe, A. Alwithenani, D. Bethune, M. Castonguay, A. Drucker, G. Flowerdew, et al., Molecular profiling of non-small cell lung cancer, PLoS One 15 (8) (2020), e0236580.
[3] T.J. Lynch, D.W. Bell, R. Sordella, S. Gurubhagavatula, R.A. Okimoto, B. W. Brannigan, et al., Activating mutations in the epidermal growth factor receptor underlying responsiveness of non-small-cell lung cancer to gefitinib, N. Engl. J. Med. 350 (21) (2004) 2129–2139.
[4] A.R. Li, D. Chitale, G.J. Riely, W. Pao, V.A. Miller, M.F. Zakowski, et al., EGFR Mutations in Lung Adenocarcinomas: clinical testing experience and relationship to EGFR gene copy number and immunohistochemical expression, J. Mol. Diagn. 10 (3) (2008) 242–248.
[5] M.H. Cohen, G.A. Williams, R. Sridhara, G. Chen, R. Pazdur, FDA drug approval summary: Gefitinib (ZD1839) (Iressa®) tablets, Oncologist 8 (4) (2003) 303–306.
[6] J.G. Paez, P.A. Jänne, J.C. Lee, S. Tracy, H. Greulich, S. Gabriel, et al., EGFR mutations in lung cancer: correlation with clinical response to gefitinib therapy, Science 304 (5676) (2004) 1497–1500.
[7] S. Kobayashi, T.J. Boggon, T. Dayaram, P.A. Jänne, O. Kocher, M. Meyerson, et al., EGFR mutation and resistance of non–small-cell lung cancer to Gefitinib, N. Engl. J. Med. 352 (8) (2009) 786–792.
[8] M.R.V. Finlay, M. Anderton, S. Ashton, P. Ballard, P.A. Bethel, M.R. Box, et al., Discovery of a potent and selective EGFR inhibitor (AZD9291) of both sensitizing and T790M resistance mutations that spares the wild type form of the receptor, J. Med. Chem. 57 (20) (2014) 8249–8267.
[9] S.L. Greig, Osimertinib: first global approval, Drugs 76 (2) (2016) 263–273.
[10] K.S. Thress, C.P. Paweletz, E. Felip, B.C. Cho, D. Stetson, B. Dougherty, et al., Acquired EGFR C797S mutation mediates resistance to AZD9291 in non–small cell lung cancer harboring EGFR T790M, Nat. Med. 21 (6) (2015) 560–562.
[11] A.A. Zulkifli, F.H. Tan, T.L. Putoczki, S.S. Stylli, R.B. Luwor, STAT3 signaling mediates tumour resistance to EGFR targeted therapeutics, Mol. Cell Endocrinol. 451 (2017) 15–23.
[12] Q. Wang, S. Yang, K. Wang, S.Y. Sun, MET inhibitors for targeted therapy of EGFR TKI-resistant lung cancer, J. Hematol. Oncol. 12 (1) (2019) 63.
[13] A.B. Cortot, C.E. Repellin, T. Shimamura, M. Capelletti, K. Zejnullahu, D. Ercan, et al., Resistance to irreversible EGF receptor tyrosine kinase inhibitors through a multistep mechanism involving the IGF1R pathway, Cancer Res. 73 (2) (2013) 834–843.
[14] Q. Liu, S. Yu, W. Zhao, S. Qin, Q. Chu, K. Wu, EGFR-TKIs resistance via EGFR-independent signaling pathways, Mol. Cancer 17 (1) (2018) 53.
[15] H. Taniguchi, T. Yamada, R. Wang, K. Tanimura, Y. Adachi, A. Nishiyama, et al., AXL confers intrinsic resistance to osimertinib and advances the emergence of tolerant cells, Nat. Commun. 10 (1) (2019) 259.
[16] K. Ohashi, L.V. Sequist, M.E. Arcila, T. Moran, J. Chmielecki, Y.L. Lin, et al., Lung cancers with acquired resistance to EGFR inhibitors occasionally harbor BRAF gene

mutations but lack mutations in KRAS, NRAS, or MEK1, Proc. Natl. Acad. Sci. USA 109 (31) (2012) E2127–E2133.
[17] L.V. Sequist, B.A. Waltman, D. Dias-Santagata, S. Digumarthy, A.B. Turke, P. Fidias, et al., Genotypic and histological evolution of lung cancers acquiring resistance to EGFR inhibitors, Sci. Transl. Med. 3 (75) (2011) 75ra26.
[18] S. Singh, S. Chellappan, Lung cancer stem cells: molecular features and therapeutic targets, Mol. Asp. Med. 39 (2014) 50–60.
[19] Y. Yu, G. Ramena, R.C. Elble, The role of cancer stem cells in relapse of solid tumors, Front. Biosci. 1 (4) (2012) 1528.
[20] J. Wang, Z. hong Li, J. White, L. bo Zhang, Lung cancer stem cells and implications for future therapeutics, Cell Biochem. Biophys. 69 (3) (2014) 389–398.
[21] D. Hanahan, R.A. Weinberg, Hallmarks of cancer: the next generation, Cell 144 (5) (2011) 646–674.
[22] L.S.S. Pulla, S. Begum Ahil, Review on target domains and natural compound-based inhibitors of fatty acid synthase for anticancer drug discovery, Chem. Biol. Drug Des. 98 (5) (2021) 869–884.
[23] A. Ali, E. Levantini, J.T. Teo, J. Goggi, J.G. Clohessy, C.S. Wu, et al., Fatty acid synthase mediates EGFR palmitoylation in EGFR mutated non-small cell lung cancer, EMBO Mol. Med. 10 (2018) 1–19.
[24] E. Polonio-Alcalá, S. Palomeras, D. Torres-Oteros, J. Relat, M. Planas, L. Feliu, et al., Fatty acid synthase inhibitor G28 shows anticancer activity in EGFR tyrosine kinase inhibitor resistant lung adenocarcinoma models, Cancers 12 (5) (2020) 1–18.
[25] N. Zhan, B. Li, X. Xu, J. Xu, S. Hu, Inhibition of FASN expression enhances radiosensitivity in human non-small cell lung cancer, Oncol. Lett. 15 (4) (2018) 4578.
[26] R. Ventura, K. Mordec, J. Waszczuk, Z. Wang, J. Lai, M. Fridlib, et al., Inhibition of de novo palmitate synthesis by fatty acid synthase induces apoptosis in tumor cells by remodeling cell membranes, inhibiting signaling pathways, and reprogramming gene expression, EBioMedicine 2 (8) (2015) 808.
[27] L. Yang, F. Zhang, X. Wang, Y. Tsai, K.H. Chuang, P.C. Keng, et al., A FASN-TGF-β1-FASN regulatory loop contributes to high EMT/ metastatic potential of cisplatin-resistant non-small cell lung cancer, Oncotarget 7 (34) (2016) 55543–55554.
[28] K. Jacobsen, J. Bertran-Alamillo, M.A. Molina, C. Teixidó, N. Karachaliou, M. H. Pedersen, et al., Convergent Akt activation drives acquired EGFR inhibitor resistance in lung cancer, Nat. Commun. 8 (1) (2017) 410.
[29] T.C. Chou, P. Talalay, Quantitative analysis of dose-effect relationships: the combined effects of multiple drugs or enzyme inhibitors, Adv. Enzym. Regul. 22 (C) (1984) 27–55.
[30] J. Crous-Masó, S. Palomeras, J. Relat, C. Camó, Ú. Martínez-Garza, M. Planas, et al., (−)-Epigallocatechin 3-gallate synthetic analogues inhibit fatty acid synthase and show anticancer activity in triple negative breast cancer, Molecules 23 (5) (2018) 1160.
[31] M. Sankaranarayanapillai, N. Zhang, K.A. Baggerly, J.G. Gelovani, Metabolic shifts induced by fatty acid synthase inhibitor orlistat in non-small cell lung carcinoma cells provide novel pharmacodynamic biomarkers for positron emission tomography and magnetic resonance spectroscopy, Mol. Imaging Biol. 15 (2) (2013) 136–147.
[32] L. Chang, S. Fang, Y. Chen, Z. Yang, Y. Yuan, J. Zhang, et al., Inhibition of FASN suppresses the malignant biological behavior of non-small cell lung cancer cells via deregulating glucose metabolism and AKT/ERK pathway, Lipids Health Dis. 18 (1) (2019) 118.
[33] Y. Yan, Y. Zhou, J. Li, Z. Zheng, Y. Hu, L. Li, et al., Sulforaphane downregulated fatty acid synthase and inhibited microtubule-mediated mitophagy leading to apoptosis, Cell Death Dis 12 (10) (2021) 917.
[34] V.M. Youngblood, L.C. Kim, D.N. Edwards, Y. Hwang, P.R. Santapuram, S. M. Stirdivant, et al., The ephrin-A1/EPHA2 signaling axis regulates glutamine metabolism in HER2-positive breast cancer, Cancer Res 76 (7) (2016) 1825.
[35] J.A. Menendez, R. Lupu, Fatty acid synthase: a druggable driver of breast cancer brain metastasis, Expert Opin. Ther. Targets 26 (5) (2022) 427–444.
[36] B. Griffiths, C.A. Lewis, K. Bensaad, S. Ros, Q. Zhang, E.C. Ferber, et al., Sterol regulatory element binding protein-dependent regulation of lipid synthesis supports cell survival and tumor growth, Cancer Metab 1 (1) (2013) 3.
[37] F. Shi, C. Wang, L. Wang, X. Song, H. Yang, Q. Fu, et al., Preparative isolation and purification of steroidal glycoalkaloid from the ripe berries of Solanum nigrum L. by preparative HPLC–MS and UHPLC–TOF-MS/MS and its anti-non-small cell lung tumors effects in vitro and in vivo, J. Sep Sci. 42 (15) (2019) 2471–2481.
[38] H. Orita, J. Coulter, C. Lemmon, E. Tully, A. Vadlamudi, S.M. Medghalchi, et al., Selective inhibition of fatty acid synthase for lung cancer treatment, Clin. Cancer Res. 13 (23) (2007) 7139–7145.
[39] J. Relat, A. Blancafort, G. Oliveras, S. Cufí, D. Haro, P.F. Marrero, et al., Different fatty acid metabolism effects of (-)-Epigallocatechin-3-Gallate and C75 in Adenocarcinoma lung cancer, BMC Cancer 12 (2012) 280.
[40] A. Giró-Perafita, S. Palomeras, D.H. Lum, A. Blancafort, G. Viñas, G. Oliveras, et al., Preclinical evaluation of fatty acid synthase and EGFR inhibition in triple-negative breast cancer, Clin. Cancer Res. 22 (18) (2016) 4687–4697.
[41] M.J. Sanaei, S. Razi, A. Pourbagheri-Sigaroodi, D. Bashash, The PI3K/Akt/mTOR pathway in lung cancer; oncogenic alterations, therapeutic opportunities, challenges, and a glance at the application of nanoparticles, Transl. Oncol. 18 (2022) 101364.
[42] T. Ninomiya, N. Takigawa, E. Ichihara, N. Ochi, T. Murakami, Y. Honda, et al., Afatinib prolongs survival compared with gefitinib in an epidermal growth factor receptor-driven lung cancer model, Mol. Cancer Ther. 12 (5) (2013) 589–597.
[43] H.Y. Lin, S.C. Hou, S.C. Chen, M.C. Kao, C.C. Yu, S. Funayama, et al., (-)-Epigallocatechin gallate induces Fas/CD95-mediated apoptosis through inhibiting constitutive and IL-6-induced JAK/STAT3 signaling in head and neck squamous cell carcinoma cells, J. Agric. Food Chem. 60 (10) (2012) 2480–2489.
[44] S.N. Tang, J. Fu, S. Shankar, R.K. Srivastava, EGCG enhances the therapeutic potential of gemcitabine and CP690550 by inhibiting STAT3 signaling pathway in human pancreatic cancer, PLoS One 7 (2) (2012) e31067.
[45] Y. Geng, Y. Zhou, S. Wu, Y. Hu, K. Lin, Y. Wang, et al., Sulforaphane induced apoptosis via promotion of mitochondrial fusion and ERK1/2-mediated 26S proteasome degradation of novel pro-survival bim and upregulation of bax in human non-small cell lung cancer cells, J. Cancer 8 (13) (2017) 2456.
[46] X. Wu, L. Qin, V. Fako, J.T. Zhang, Molecular mechanisms of fatty acid synthase (FASN)-mediated resistance to anti-cancer treatments, Adv. Biol. Regul. 54 (1) (2014) 214–221.
[47] B.M. Ku, J.Y. Heo, J. Kim, J.M. sun, S.H. Lee, J.S. Ahn, et al., ERK inhibitor ASN007 effectively overcomes acquired resistance to EGFR inhibitor in non-small cell lung cancer, Invest New Drugs 40 (2) (2022) 265–273.
[48] W. Khan, D. Augustine, R. Rao, S. Patil, K. Awan, S. Sowmya, et al., Lipid metabolism in cancer: a systematic review, J. Carcinog. 20 (1) (2021) 4.
[49] A. Giró-Perafita, M. Rabionet, M. Planas, L. Feliu, J. Ciurana, S. Ruiz-Martínez, et al., EGCG-derivative G28 shows high efficacy inhibiting the mammosphere-forming capacity of sensitive and resistant TNBC models, Molecules 24 (6) (2019) 1–15.
[50] M. Rabionet, E. Polonio-Alcalá, J. Relat, M. Yeste, J. Sims-Mourtada, A.M. Kloxin, et al., Fatty acid synthase as a feasible biomarker for triple negative breast cancer stem cell subpopulation cultured on electrospun scaffolds, Mater. Today Bio 12 (2021), 100155.
[51] L. Li, C.C. Liu, X. Chen, S. Xu, S.H. Cortes-Manno, S.H. Cheng, Mechanistic study of bakuchiol-induced anti-breast cancer stem cell and in vivo anti-metastasis effects, Front. Pharmacol. 8 (2017) 746.
[52] M.T.E. Montales, R.C.M. Simmen, E.S. Ferreira, V.A. Neves, F.A. Simmen, Metformin and soybean-derived bioactive molecules attenuate the expansion of stem cell-like epithelial subpopulation and confer apoptotic sensitivity in human colon cancer cells, Genes Nutr 10 (6) (2015) 49.
[53] H. Dianat-Moghadam, M. Khalili, M. Keshavarz, M. Azizi, H. Hamishehkar, R. Rahbarghazi, et al., Modulation of LXR signaling altered the dynamic activity of human colon adenocarcinoma cancer stem cells in vitro, Cancer Cell Int 21 (1) (2021) 100.
[54] L. Yang, P. Shi, G. Zhao, J. Xu, W. Peng, J. Zhang, et al., Targeting cancer stem cell pathways for cancer therapy, Signal Transduct. Target Ther. 5 (1) (2020) 8.
[55] R. Rosell, T. Moran, C. Queralt, R. Porta, F. Cardenal, C. Camps, et al., Screening of epidermal growth factor receptor mutation in lung cancer, N. Engl. J. Med. 361 (2009) 958–967.
[56] H. Orita, J. Coulter, E. Tully, F.P. Kuhajda, E. Gabrielson, Inhibiting fatty acid synthase for chemoprevention of chemically induced lung tumors, Clin. Cancer Res. 14 (8) (2008) 2458–2464.
[57] P. Visca, V. Sebastiani, C. Botti, M.G. Diodoro, R.P. Lasagni, F. Romagnoli, et al., Fatty Acid Synthase (FAS) is a marker of increased risk of recurrence in lung carcinoma, Anticancer Res. 24 (6) (2004) 4169–4173.
[58] Y. Wang, X. Zhang, W. Tan, J. Fu, W. Zhang, Significance of fatty acid synthase expression in non-small cell lung cancer, Zhonghua Zhong Liu Za Zhi 3 (24) (2002) 271–273.
[59] D. Cerne, I. Prodan Zitnik, M. Sok, Increased fatty acid synthase activity in non-small cell lung cancer tissue is a weaker predictor of shorter patient survival than increased lipoprotein lipase activity, Arch. Med. Res. 41 (6) (2010) 405–409.
[60] L.R. Bollu, R.R. Katreddy, A.M. Blessing, N. Pham, B. Zheng, X. Wu, et al., Intracellular activation of EGFR by fatty acid synthase dependent palmitoylation, Oncotarget 6 (33) (2015) 34992–35003.